Adaptive Controller Placement for Wireless Sensor-Actuator Networks with Erasure Channels

Daniel E. Quevedo, Karl H. Johansson, Anders Ahlén, and Isabel Jurado

Abstract—**Wireless sensor-actuator networks offer flexibility for control design. One novel element which may arise in networks with multiple nodes is that the role of some nodes does not need to be fixed. In particular, there is no need to pre-allocate which nodes assume controller functions and which ones merely relay data. We present a flexible architecture for networked control using multiple nodes connected in series over analog erasure channels without acknowledgments. The control architecture proposed adapts to changes in network conditions, by allowing the role played by individual nodes to depend upon transmission outcomes. We adopt stochastic models for transmission outcomes and characterize the distribution of controller location and the covariance of system states. Simulation results illustrate that the proposed architecture has the potential to give better performance than limiting control calculations to be carried out at a fixed node.**

I. INTRODUCTION

In a Networked Control System (NCS), sensor, controller and actuator links are not transparent, but are affected by bit-rate limitations, packet dropouts and/or delays. This leads to performance degradation and makes the design of NCSs often a challenging task [2], [3]. An interesting aspect is that, when compared to traditional hard-wired control loops, wireless NCSs offer architectural flexibility and additional degrees of freedom. Whilst sensor and actuator functionalities will generally be pre-allocated, often there is no need to pre-assign in a static fashion which nodes carry out control calculations, and which nodes merely relay data. Intuitively, the roles of individual nodes should depend on the information available at each time instant. In the present work, we examine this question for the case of NCSs with random packet dropouts. Our motivating application is real-time control in the process industry. Several new standards have recently been introduced for multi-hop wireless sensor and actuator networks, e.g., WirelessHART, ISA-100, and this paper proposes a new adaptive controller placement suitable to be implemented over these standards. Note that the plant time constants in process industry are often of the order of seconds or minutes (or

Daniel Quevedo is with the School of Electrical Engineering & Computer Science, The University of Newcastle, NSW 2308, Australia; dquevedo@ieee.org. Karl H. Johansson is with ACCESS Linnaeus Centre, School of Electrical Engineering, Royal Institute of Technology, Stockholm, Sweden; kallej@ee.kth.se. Anders Ahlén is with Signals and Systems, Uppsala University, SE-751 21, Uppsala, Sweden; Anders.Ahlen@signal.uu.se. Isabel Jurado is with the Departamento de Ingeniería de Sistemas y Automática, Escuela Superior de Ingenieros, Universidad de Sevilla, Spain. ijurado@cartuja.us.es

even higher), so we make the reasonable assumption that network-induced delays can be neglected. As background to our current work, [4] studies performance of three static NCS architectures by adopting an additive signal-to-noise ratio constrained channel model. The results in [4] suggest that, in the absence of coding, placing the controller at the actuator node will give better performance than placing it at the sensor node. The work [5] examines NCSs with stochastic packet dropouts using optimal control techniques. *Inter-alia*, the work shows that optimal performance can be achieved if all nodes aggregate their entire history of received data and relay it to the controller-actuator. Depending upon the information available at each node, various optimal control problems can be analyzed. More recently, [6] investigates a distributed control strategy wherein the network itself acts as a controller for a MIMO plant. All nodes (including the actuator nodes) perform linear combinations of internal state variables of neighboring nodes. In the case of analog erasure channels with i.i.d. dropouts (without acknowledgments), in [6] the resulting NCS is then cast, analyzed and designed as a jump-linear system.

The present work studies a single-loop NCS topology which uses a series connection of analog erasure channels. We focus on situations where the wireless nodes have only limited energy and processing power, precluding long data packets. Further, the nodes do not provide local transmission acknowledgments. Feedback (or acknowledgment) is only provided by the actuator node, which broadcasts the applied plant input value over parallel unreliable links to the intermediate nodes. This strategy is plausible as the actuator node is powered, which is a reasonable assumption for most actuators in process industry. Due to random dropouts, the actuator node does not have full information on plant outputs. This constitutes one of the major difficulties when implementing a controller in such a NCS. We address this issue by using an estimation and control structure which is distributed across the network. Instead of tackling optimal control formulations (which depend upon network parameters and may therefore be difficult to implement in practice), we adopt a so-called emulation-based approach, where the controller has been pre-designed; see, e.g., [7], [8], [9]. To be more specific, we assume that the control policy consists of a pre-designed state feedback-gain combined with a state observer, which, in the absence of network effects, would lead to the desired performance. Within this context, we present a flexible NCS architecture where the role played by individual nodes depends upon transmission outcomes. While all nodes calculate local state estimates at all times, with the algorithm proposed, transmission outcomes determine, at each instant, whether the control input will be

Fig. 1. Single-loop control over a wireless sensor-actuator network: forward- and feedback-links are unreliable.

calculated at the actuator node, at the sensor node or at one of the intermediate nodes. It turns out that, if individual dropout processes are i.i.d., then the controller location has a stationary distribution, which can be easily characterized. To analyze the performance of the dynamic NCS architecture in the presence of correlated dropouts, we derive a jump-linear system model and adopt the network model recently introduced in [10]. This model encompasses temporal and spatial correlations of packet dropouts and is therefore of more practical importance than more traditional i.i.d. models. The present paper goes beyond our recent conference contribution [11], by presenting a closed loop model and considering networks with correlated dropouts. Our approach complements [11] by focusing on a nominal linear estimator, as opposed to a time-varying Kalman filter. This opens the possibility to analyze NCS performance with correlated dropouts using techniques from jump-linear systems.

This paper is organized as follows. Section II describes the NCS topology of interest. In Section III we present the dynamic NCS architecture. For the case of independent dropouts, Section IV provides the distribution of the controller location. Section V derives an overall closed loop model. Performance issues are studied in Section VI. Section VII documents simulation studies. Section VIII draws conclusions.

Notation: We write $\mathbb{N}_0$ for $\{0, 1, 2, \ldots\}$; $\mathbb{R}$ are the real numbers, whereas $\mathbb{R}_{\geq 0} \triangleq [0, \infty)$. The ℓ-th unit row-vector in Euclidean space is denoted e_ℓ, for example, $e_2 = \begin{bmatrix} 0 & 1 & 0 & \ldots & 0 \end{bmatrix}$; I_n is the $n \times n$ unit matrix, $0_n \triangleq 0 \cdot I_n$; $\otimes$ refers to the Kronecker product. For any set of column vectors, $\{u_1, \ldots, u_n\}$, $\operatorname{col}(u_1, \ldots, u_n) = [u_1^T, \ldots, u_n^T]^T$. We adopt the convention $\sum_{j=1}^{0} a_j = 0$, for all $a_0, a_1 \in \mathbb{R}$. A real random variable μ, which is zero-mean Gaussian with covariance Γ is denoted by $\mu \sim \mathcal{N}(0, \Gamma)$.

II. WIRELESS SENSOR-ACTUATOR NETWORK SETUP

We consider MIMO LTI plant models of the form

$$\begin{aligned} x_{k+1} &= Ax_k + Bu_k + w_k \\ y_k &= Cx_k + v_k, \quad k \in \mathbb{N}_0 \end{aligned} \tag{1}$$

where $x_0 \sim \mathcal{N}(\bar{x}_0, P_0)$, $P_0 \succ 0$. In (1), $u_k \in \mathbb{R}^m$ is the plant input, $x_k \in \mathbb{R}^n$ is the state, $y_k \in \mathbb{R}^p$ is the output, and $w_k \sim \mathcal{N}(0, Q)$, $Q \succ 0$ and $v_k \sim \mathcal{N}(0, R)$, $R \succ 0$, are driving noise and measurement noise, respectively. As foreshadowed in the introduction, we focus on a situation where suitable

feedback and estimator gains $L \in \mathbb{R}^{m \times n}$ and $K \in \mathbb{R}^{n \times p}$ have been pre-designed for a situation where the controller (K, L) has perfect access to plant outputs and inputs. Consequently, we assume that if the control inputs

$$u_k = L\hat{x}_k^{\text{nom}}, \quad k \in \mathbb{N}_0, \quad \text{with} \tag{2}$$

$$\hat{x}_k^{\text{nom}} = A\hat{x}_{k-1}^{\text{nom}} + Bu_{k-1} + K(y_k - C(A\hat{x}_{k-1}^{\text{nom}} + Bu_{k-1})), \tag{3}$$

where $\hat{x}_k^{\text{nom}}$ denotes an estimate of the state x_k, were implemented at the plant, then satisfactory performance would be attained. The main theme of the present work is to investigate how to implement the above nominal controller, when using a wireless sensor-actuator network with dropouts.

The sensor node measures the plant output y_k, whereas the actuator node manipulates the plant input u_k. The loop is closed over a wireless network, characterised via a (directed) line-graph having M nodes, see Fig. 1. Transmissions are in sequential Round-Robin fashion $\{1, 2, \ldots, M, 1, 2, \ldots\}$ as depicted in Fig. 2. More precisely, the packet $s_k^{(i)}$ is transmitted from node i to node $i+1$ at times $kT + i\tau$, where T is the sampling period of (1) and $\tau \ll T/(M+1)$ refers to the times between transmissions of packets $s_k^{(i)}$. The input u_k is applied at time $kT + (M+1)\tau$. We thus assume that in-network processing is much faster than the plant dynamics (1) and neglect delays introduced by the network.

The network introduces stochastic packet dropouts. To study the situation, we adopt an analog erasure channel model and introduce the binary success processes

$$\gamma_k^{(i)} \in \{0, 1\}, \quad k \in \mathbb{N}_0, \ i \in \{1, 2, \ldots, M-1\},$$

where $\gamma_k^{(i)} = 1$ indicates that transmission of the packet $s_k^{(i)}$ from node i to node $i+1$ at time $kT + i\tau$, is successful, i.e., error-free; $\gamma_k^{(i)} = 0$ refers to a packet-dropout. Throughout this work, we assume that transmission outcomes are known at the corresponding receiver sides and that the sensor node $i = 1$ has direct access to plant output measurements. For notational convenience, we write $\gamma_k^{(0)} = 1$, for all $k \in \mathbb{N}_0$. To save energy, the wireless nodes $i \in \{1, 2, \ldots, M-1\}$ do not provide acknowledgments of receipt of the packets. The actuator node M provides a feedback mechanism: At time $(k+1)T - \tau$, it broadcasts the control value u_k to nodes $i \in \{1, \ldots, M-1\}$, see Fig. 1. Due to channel fading, the *feedback links* between actuator and sensors are also affected by dropouts. We denote the associated success processes via

$$\delta_k^{(i)} \in \{0, 1\}, \quad k \in \mathbb{N}_0, \ i \in \{1, 2, \ldots, M-1\}.$$

More precisely, if u_k is successfully received at node i, then we set $\delta_k^{(i)} = 1$; see also [12] for studies on the importance of acknowledgments in closed loop control. We assume that the actuator node has perfect knowledge of plant inputs, and thus, write $\delta_k^{(M)} = 1$, $\forall k \in \mathbb{N}_0$. Since the actuator node will, in general, have less stringent energy constraints than the other nodes, we focus our attention on situations where the feedback links are more reliable than the forward links moving data from the sensor to the actuator.

Due to packet dropouts, plant output measurements are not always available at the actuator node. On the other hand, the
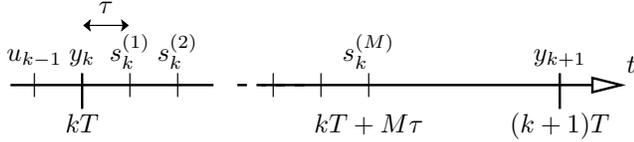
Fig. 2. TDMA Transmission Schedule. The plant input u_k is applied at time $kT + M\tau$ and broadcast at time $(k+1)T - \tau$.

sensor node will, in general, not have perfect information of previous plant inputs. This makes the implementation of the nominal controller (2)–(3) a challenging task. In the sequel, we will present an adaptive controller placement algorithm where the computations leading to the plant inputs are distributed across the network. We foresee that our approach will lead to a dynamic assignment of the role played by the individual network nodes. As will become apparent in the sequel, which tasks are carried out by individual nodes at each time instant, will depend upon transmission outcomes.

III. FLEXIBLE CONTROLLER PLACEMENT

To keep communication overheads low, the packets transmitted by each node i have only two fields, namely, output measurements and tentative plant inputs (if available):

$$s_k^{(i)} = \left(y_k, u_k^{(i)}\right). \qquad (4)$$

Plant outputs are transmitted in order to pass on information on the plant state to the nodes $\{i+1, i+2, \ldots, M\}$, see Fig. 1. On the other hand, $u_k^{(i)}$ in (4) is the plant input which is applied at the plant provided the packet $s_k^{(i)}$ is delivered at the actuator node. If $s_k^{(i)}$ is lost, then following the algorithm described below, the plant input will be provided by one of the later nodes $\ell > i$, which thereby takes on the controller role at time k. In the sequel, we will refer to the node which calculates the plant input at time k as $c_k \in \{1, 2, \ldots, M\}$:

$$u_k = L\hat{x}_k^{(c_k)}, \quad k \in \mathbb{N}_0, \qquad (5)$$

where $\hat{x}_k^{(c_k)}$ is the local plant state estimate computed at node c_k. Intuitively, good control performance will be achieved if the estimate used in (5) is accurate. Clearly, due to the multi-hop nature of the network, nodes which are closer to the sensor will have access to more output measurements, see Fig. 1. On the other hand, one can expect that nodes which are physically located closer to the actuator node will on average receive more plant input acknowledgments, thus, have better knowledge of plant inputs.

While only the node c_k will provide u_k, in our formulation all nodes compute local state estimates, $\hat{x}_k^{(i)}$, by using the data received from the actuator node and the preceding node. This serves as safeguard for instances when the loop is broken due to dropouts. Motivated by the fact that often feedback links from the actuator to the intermediate sensors are "quite reliable", we adopt the following simple procedure: If plant output measurements are available at node i, then state estimators are of the form (3); at instances when the plant input

is not available, an open loop estimate is used, thus:

$$\hat{x}_k^{(i)} = A\hat{x}_{k-1}^{(i)} + B\hat{u}_{k-1}^{(i)} + K_k^{(i)}\left(y_k - C(A\hat{x}_{k-1}^{(i)} + B\hat{u}_{k-1}^{(i)})\right), \qquad (6)$$

where

$$K_k^{(i)} \triangleq \Gamma_k^{(i)} K, \quad \text{and} \quad \Gamma_k^{(i)} \triangleq \prod_{j \in \{0, 1, \ldots, i-1\}} \gamma_k^{(j)} \qquad (7)$$

is equal to 1 if and only if y_k is available at node i at time $kT + (i-1)\tau$. In (6), $\hat{u}_{k-1}^{(i)}$ is a local plant input estimate. In particular, if $\delta_{k-1}^{(i)} = 1$, then $\hat{u}_{k-1}^{(i)} = u_{k-1}$. At instances where $\delta_{k-1}^{(i)} = 0$, node i uses $u_{k-1}^{(i)}$, the tentative plant input value transmitted in the second field of the previous packet $s_{k-1}^{(i)}$ (if non-empty), or otherwise sets $\hat{u}_{k-1}^{(i)} = L\hat{x}_{k-1}^{(i)}$. More details on the estimator are given in Section V.

Remark 1: Of course, the above transmission and control strategy will in general not be optimal. In particular, nodes do not transmit local state estimates and the control law does not depend upon network parameters, e.g., dropout probabilities; cf., [13]. The aim of the present work is to develop a simple and practical method, which uses an existing control and estimation policy for implementation over an unreliable network and only requires little communication. □

Remark 2: In [11], instead of using (7), the gains $K_k^{(i)}$ were taken as the Kalman filter gains for a system with intermittent observations, see, e.g., [14], [15], [16]. Our subsequent analysis up to (22) can be applied to this structure as well. However, the jump-linear model derived in Section V requires a jump-linear estimation model, such as (7). □

Algorithm 1, run at every node $i \in \{1, 2, \ldots, M\}$, embodies the adaptive controller allocation method described in the preceding section. Which calculations are carried out at each node, depends upon transmission outcomes involving the current node (see lines 6, 8, 14, 24 and 37) and also transmission outcomes at previous nodes (see lines 16, 19 and 24). In particular, node i only calculates a tentative plant input when no tentative plant input is received from node $i-1$ and node i has successfully received u_{k-1} (see lines 9 and 25). Therefore, preference is given to relay incoming tentative plant input values. The reason for adopting this decision procedure lies in that we assume that data sent from the actuator node to intermediate nodes is often available, whereas transmissions of packets $s_k^{(i)}$ are less reliable. Thus, nodes closer to the sensor node can be expected to have better state estimates than nodes located further down the line. In particular, the sensor node $i = 1$ uses as input

$$s_k^{(0)} = (y_k, \emptyset), \quad \gamma_k^{(0)} = 1. \qquad (8)$$

If $\delta_{k-1}^{(1)} = 1$, then the sensor node calculates a tentative control value and transmits $s_k^{(1)} = (y_k, L\hat{x}_k^{(1)})$ to node 2. Subsequent nodes relay this packet towards the actuator node. If the packet is dropped along the way, then the next node i where $\delta_{k-1}^{(i)} = 1$, calculates a tentative control $u_k^{(i)} = L\hat{x}_k^{(i)}$ and transmits $s_k^{(i)} = (\emptyset, u_k^{(i)})$ to node $i+1$, etc. On the other hand, if $\delta_{k-1}^{(1)} = 0$, then $s_k^{(0)}$ is relayed to subsequent nodes until arriving at some node i where u_{k-1} was successfully received. Control calculations

Algorithm 1 Adaptive Controller Placement

1: $k \leftarrow 0$, $\hat{x}_0^{(i)} \leftarrow 0$, $j \leftarrow 0$
2: **while** $t \geq 0$ **do**   ▷ $t \in \mathbb{R}_{\geq 0}$ is actual time
3:     **while** $t \leq kT + (i-1)\tau$ **do**   ▷ wait-loop
4:         $j \leftarrow j + 1$
5:     **end while**
6:     **if** $\gamma_k^{(i-1)} = 0$ **then**   ▷ $s_k^{(i-1)}$ is dropped
7:         $\hat{u}_k^{(i)} \leftarrow L\hat{x}_k^{(i)}$
8:         **if** $\delta_{k-1}^{(i)} = 1$ **then**
9:             $s_k^{(i)} \leftarrow (\emptyset, \hat{u}_k^{(i)})$ ▷ a tentative input
10:         **else**
11:             $s_k^{(i)} \leftarrow (\emptyset, \emptyset)$
12:         **end if**
13:     **end if**
14:     **if** $\gamma_k^{(i-1)} = 1$ **then**   ▷ $s_k^{(i-1)}$ is received
15:         $(y, u) \leftarrow s_k^{(i-1)}$
16:         **if** $y \neq \emptyset$ **then**   ▷ y_k is available
17:             $\hat{x}_k^{(i)} \leftarrow \hat{x}_k^{(i)} + K(y - C\hat{x}_k^{(i)})$
18:         **end if**
19:         **if** $u \neq \emptyset$ **then**
20:             $u_k^{(i)} = u$
21:         **else**
22:             $u_k^{(i)} \leftarrow L\hat{x}_k^{(i)}$
23:         **end if**
24:         **if** $u = \emptyset \wedge \delta_{k-1}^{(i)} = 1$ **then**
25:             $s_k^{(i)} \leftarrow (y, u_k^{(i)})$ ▷ a tentative input
26:         **else**
27:             $s_k^{(i)} \leftarrow (y, u)$ ▷ $s_k^{(i-1)}$ is forwarded
28:         **end if**
29:     **end if**
30:     **while** $t < kT + i\tau$ **do**   ▷ wait-loop
31:         $j \leftarrow j + 1$
32:     **end while**
33:     **transmit** $s_k^{(i)}$
34:     **while** $t \leq (k+1)T - \tau$ **do**   ▷ wait-loop
35:         $j \leftarrow j + 1$
36:     **end while**
37:     **if** $\delta_k^{(i)} = 1$ **then**   ▷ u_k is available
38:         $\hat{x}_{k+1}^{(i)} \leftarrow A\hat{x}_k^{(i)} + Bu_k$
39:     **else**   ▷ the value in $s_k^{(i)}$ is used
40:         $\hat{x}_{k+1}^{(i)} \leftarrow A\hat{x}_k^{(i)} + Bu_k^{(i)}$
41:     **end if**
42:     $k \leftarrow k + 1$
43: **end while**

are then carried out and the packet $s_k^{(i)}$ obtained is relayed towards the actuator node, etc. The actuator node implements $u_k = u_k^{(M)}$, the value contained in the second field of $s_k^{(M)}$.

Remark 3: An advantage of allowing the control calculations to be located arbitrarily and in a time-varying fashion, is that it makes more difficult for someone to attack the NCS. The development of secure control strategies based on Algorithm 1 presented remains a topic of future research.   □

IV. DYNAMIC CONTROLLER LOCATION

With Algorithm 1, which of the nodes calculates the plant input u_k, depends upon the transmission outcomes. For further reference, we shall denote the set of nodes which calculate a tentative control input (see lines 9 and 25 of Algorithm 1) via $\mathcal{C}_k \subset \{1, 2, \ldots, M\}$. It is convenient to introduce the processes $\{\mu_k^{(i)}\}$, and $\{c_k^{(i)}\}$, where $i \in \{0, 1, \ldots, M\}$ and

$$\mu_k^{(i)} \triangleq \begin{cases} 0 & \text{if the second field of } s_k^{(i)} \text{ is empty,} \\ 1 & \text{otherwise,} \end{cases} \tag{9}$$
$$c_k^{(i)} \triangleq \mu_k^{(i)} \max(\mathcal{C}_k \cap \{1, 2, \ldots, i\}).$$

Note that $\mu_k^{(1)} = \delta_{k-1}^{(1)}, \forall k \in \mathbb{N}$. If $c_k^{(i)} > 0$, then $c_k^{(i)}$ denotes the node where the second field of $s_k^{(i)}$ was calculated. It is easy to see that, with the algorithm proposed and since the packets $s_k^{(i)}$ are communicated sequentially, see Fig. 2, we have $c_k^{(1)} = \delta_{k-1}^{(1)}$, for all $k \in \mathbb{N}_0$, whereas

$$c_k^{(i)} = \begin{cases} i\delta_{k-1}^{(i)} & \text{if } c_k^{(i-1)} = 0 \vee \gamma_k^{(i-1)} = 0, \\ c_k^{(i-1)} & \text{if } c_k^{(i-1)} > 0 \wedge \gamma_k^{(i-1)} = 1, \end{cases} \tag{10}$$

for $i \in \{2, \ldots, M\}$, $k \in \mathbb{N}_0$. The "controller node at time k", i.e., the node where u_k was calculated is given by

$$c_k \triangleq c_k^{(M)} = \max(\mathcal{C}_k), \quad \forall k \in \mathbb{N}_0, \tag{11}$$

see (5). To derive our results, we introduce the aggregated transmission outcome process $\{\beta_k\}$, $k \in \mathbb{N}_0$, where

$$\beta_k \triangleq \sum_{i=1}^{M-1} (2^{M-1}\gamma_{k+1}^{(i)} + \delta_k^{(i)})2^{i-1}, \quad k \in \mathbb{N}_0. \tag{12}$$

Note that $\beta_{k-1} \in \mathbb{I} \triangleq \{0, 1, \ldots, 2^{2M-2} - 1\}$ collects the outcomes of all transmissions which occur during the time-interval $[kT - \tau, kT + M\tau]$, see Fig. 2. Thus, β_{k-1} determines $\mathcal{C}_k$ and c_k, i.e., the controller location will dynamically adapt to the network conditions. To further elucidate the situation, in the sequel we will regard $\{\beta_k\}$, $k \in \mathbb{N}_0$ as a stochastic process. We will first assume that the transmission processes are Bernoulli distributed.

Assumption 1: The link transmission processes are independent and identically distributed (i.i.d.) with a common success probability $p \in [0, 1]$:

$$\mathbf{Pr}\{\gamma_k^{(i)} = 1\} = p, \quad \forall i \in \{1, 2, \ldots, M-1\}. \tag{13}$$

The feedback link success processes are i.i.d., with

$$\mathbf{Pr}\{\delta_k^{(i)} = 1\} = q_i, \quad \forall i \in \{1, 2, \ldots, M-1\}, \tag{14}$$

for given success probabilities $q_1, q_2, \ldots, q_{M-1} \in [0, 1]$.   □
Note that while the above assumption imposes that transmission processes are i.i.d., it does take into account the fact that radio connectivity from the actuator node to the

and use (7), then (23) becomes

$$\hat{x}_{k+1}^{(i)} = \mathcal{D}^{(i)}(\beta_k)\Theta_k + \mathcal{E}^{(i)}(\beta_k)n_k,$$

$$\mathcal{D}^{(i)}(\beta_k) \triangleq \begin{bmatrix} \Gamma_{k+1}^{(i)}KCA & (I_n - \Gamma_{k+1}^{(i)}KC)(e_i \otimes A) & d_k^{(i)} \end{bmatrix}$$

$$\mathcal{E}^{(i)}(\beta_k) \triangleq \Gamma_{k+1}^{(i)}K \begin{bmatrix} C & I_p \end{bmatrix}.$$

State estimators, thus, follow the dynamic relation

$$\hat{x}_{k+1} = \mathcal{D}(\beta_k)\Theta_k + \mathcal{E}(\beta_k)n_k \quad (25)$$

$$\mathcal{D}(\beta_k) \triangleq \begin{bmatrix} \mathcal{D}^{(1)}(\beta_k) \\ \vdots \\ \mathcal{D}^{(M)}(\beta_k) \end{bmatrix}, \quad \mathcal{E}(\beta_k) \triangleq \begin{bmatrix} \mathcal{E}^{(1)}(\beta_k) \\ \vdots \\ \mathcal{E}^{(M)}(\beta_k) \end{bmatrix}.$$

On the other hand, (19) provides

$$\nu_{k+1} = \mathcal{F}(\beta_k)\Theta_k + \mathcal{G}(\beta_k)n_k, \quad (26)$$

$$\mathcal{F}(\beta_k) \triangleq \begin{bmatrix} b_{k+1}^{(1)}\mathcal{D}(\beta_k) \\ \vdots \\ b_{k+1}^{(M)}\mathcal{D}(\beta_k) \end{bmatrix}, \quad \mathcal{G}(\beta_k) \triangleq \begin{bmatrix} b_{k+1}^{(1)}\mathcal{E}(\beta_k) \\ \vdots \\ b_{k+1}^{(M)}\mathcal{E}(\beta_k) \end{bmatrix}.$$

Expressions (22), (25) and (26) lead to the jump-linear model

$$\Theta_{k+1} = \mathcal{A}(\beta_k)\Theta_k + \mathcal{B}(\beta_k)n_k, \quad (27)$$

$$\mathcal{A}(\beta_k) \triangleq \begin{bmatrix} \begin{bmatrix} A & 0_{Mn} & e_M \otimes B \end{bmatrix} \\ \mathcal{D}(\beta_k) \\ \mathcal{F}(\beta_k) \end{bmatrix}, \quad \mathcal{B}(\beta_k) \triangleq \begin{bmatrix} \begin{bmatrix} I_n & 0 \end{bmatrix} \\ \mathcal{E}(\beta_k) \\ \mathcal{G}(\beta_k) \end{bmatrix}.$$

Example 3: Consider $M = 2$, in which case $\beta_k = 2\gamma_{k+1}^{(1)} + \delta_k^{(1)}$ and $\mathbb{I} = \{0, 1, 2, 3\}$, see (12). Since $c_k^{(1)} = \delta_{k-1}^{(1)}, \delta_{k-1}^{(2)} = 1$ and $b_{k+1}^{(1)} = e_1 \otimes L$ for all $k \in \mathbb{N}_0$, (20) yields:

$$b_{k+1}^{(2)} = \begin{cases} e_2 \otimes L & \text{if } \beta_k < 3, \\ e_1 \otimes L & \text{if } \beta_k = 3. \end{cases}$$

In this case, the matrices in (25) are given by

$$\mathcal{D}(\beta_k) = \begin{bmatrix} KCA & (I_n - KC)(e_1 \otimes A) & d_k^{(1)} \\ \gamma_{k+1}^{(1)}KCA & (I_n - \gamma_{k+1}^{(1)}KC)(e_2 \otimes A) & e_2 \otimes B \end{bmatrix}$$

$$\mathcal{E}(\beta_k) = \begin{bmatrix} KC & K \\ \gamma_{k+1}^{(1)}KC & \gamma_{k+1}^{(1)}K \end{bmatrix},$$

$$d_k^{(1)} = \begin{cases} \begin{bmatrix} (I_n - KC)B & KCB \end{bmatrix} & \text{if } \beta_k \in \{0, 2\}, \\ e_2 \otimes B & \text{if } \beta_k \in \{1, 3\} \end{cases}$$

thereby, characterizing the model (27). $\square$

VI. PERFORMANCE ANALYSIS

To analyze the NCS via (27), we will adopt the stochastic modeling framework of [10]. Transmission outcome distributions depend upon the fading radio environment. To allow for temporal and spatial correlations of the radio environment (and possibly also for power and bit-rate control), in [10] we used a Markovian *network state*, $\{\Xi_k\}$, $k \in \mathbb{N}_0$, which takes values in a finite set, say $\mathbb{B}$. Each element of $\mathbb{B}$ corresponds to a possible configuration of the physical environment, e.g., position of mobile objects. Dropout probabilities of individual channels, *when conditioned on the network state*, are considered independent. In the particular instance where $\mathbb{B}$ has only
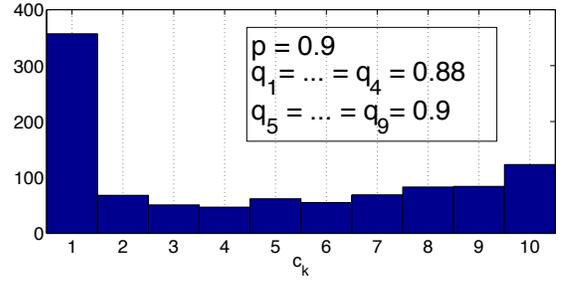
Fig. 3. Histogram of c_k for an i.i.d. network with success probabilities $p = 0.9$, $q_1 = \cdots = q_4 = 0.88$, and $q_5 = \cdots = q_9 = 0.9$.

one element, the model describes a situation with independent Bernoulli channels. For the present purposes, the model can be summarized via:

Assumption 2: The process $\{\Xi_k\}$, $k \in \mathbb{N}_0$ is an aperiodic homogeneous Markov Chain with transition probabilities $p_{ij} = \mathbf{Pr}\{\Xi_{k+1} = j \,|\, \Xi_k = i\}$, $i, j \in \mathbb{B}$ and stationary distribution $\pi_i = \lim_{k\to\infty}\mathbf{Pr}\{\Xi_k = i\}$, $i \in \mathbb{B}$. The aggregated transmission outcome process $\{\beta_k\}$ in (12) is conditionally independent given the network state $\{\Xi_k\}$, i.e., $\phi_{ij} \triangleq \mathbf{Pr}\{\beta_k = i \,|\, \Xi_k = j\}$, for all $(i, j) \in \mathbb{I} \times \mathbb{B}$. $\square$

It is worth noting that, with the above model, the process β_k is correlated, but not necessarily Markovian. However, the augmented jump process (β_k, Ξ_k), $k \in \mathbb{N}_0$ forms a finite Markov Chain. Thus, under Assumption 2, (27) belongs to the class of Markov jump-linear systems, as studied for example in [17], [18]. In particular, Theorems 3.9 and 3.33 of [17] establish necessary and sufficient conditions for mean-square stability (MSS) which can be stated in terms of feasibility of a linear-matrix inequality. The following result characterizes closed loop performance of the flexible networked control systems architecture of interest in the present work. It is tailored directly to the model in Assumption 2 without needing to resort to the augmented jump process (β_k, Ξ_k).

Theorem 1: Suppose that Assumption 2 holds, that the system (27) is MSS and define $W \triangleq \mathrm{diag}(Q, R)$,

$$\overline{\mathcal{A}}_j \triangleq \mathbf{E}\{\mathcal{A}(\beta_k) \,|\, \Xi_k = j\} = \sum_{i\in\mathbb{I}} \phi_{ij}\mathcal{A}(i), \quad j \in \mathbb{B},$$

$$\overline{\mathcal{B}}_j \triangleq \mathbf{E}\{\mathcal{B}(\beta_k) \,|\, \Xi_k = j\} = \sum_{i\in\mathbb{I}} \phi_{ij}\mathcal{B}(i), \quad j \in \mathbb{B}. \quad (28)$$

Then

$$\lim_{k\to\infty} \mathbf{E}\{\Theta_k\Theta_k^T\} = \sum_{i\in\mathbb{B}} H_i, \quad (29)$$

where H_i, $i \in \mathbb{B}$ satisfy the linear system of equations:

$$H_i = \sum_{j\in\mathbb{B}} p_{ji}\overline{\mathcal{A}}_i H_j(\overline{\mathcal{A}}_i)^T + \pi_i \overline{\mathcal{B}}_i W (\overline{\mathcal{B}}_i)^T. \quad (30)$$

In view of (24) and the fact that $u_k = \nu_k^{(M)}$, our result can be used to evaluate the plant state and input covariances.

Remark 4: By using [19, Sec.5], H_i in (30) can be written in terms of the solution to a system of linear equations. $\square$
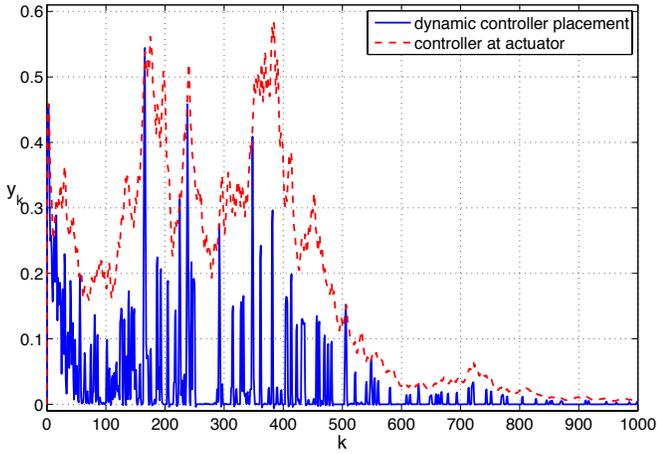
Fig. 4. Output trajectory of the plant model (33) for an i.i.d. network with success probabilities $p = 0.9$, $q_1 = \cdots = q_9 = 1$.

TABLE II
PERFORMANCE INDICES J WHEN CONTROLLING THE SYSTEM (35) OVER AN I.I.D. NETWORK WITH $q_1 = \cdots = q_4 = 0.99$, $q_5 = \cdots = q_9 = 0.995$.

p	NCS (5)–(6)	NCS (31)	NCS (32)
0.95	33.5	38.5	(unstable)
0.97	33.2	37.6	56.1
0.99	33.1	34.7	34.1

VII. SIMULATION STUDIES

We consider an NCS with $M = 10$ nodes. In addition to the implementation of the controller via Algorithm 1, we also examine two baseline NCS architectures. In the first one, the controller and estimator are fixed at the actuator node:

$$
\begin{aligned}
x_{k+1} &= Ax_k + BL\hat{x}_k^a + w_k, \\
\hat{x}_k^a &= A\hat{x}_{k-1}^a + Bu_{k-1} \\
&\quad + \Gamma_k^{(10)}K\big(y_k - C(A\hat{x}_{k-1}^a + Bu_{k-1})\big),
\end{aligned}
\tag{31}
$$

where $\Gamma_k^{(10)}$ is as in (7). In the second scheme, controller and estimator are implemented at the sensor node. If the controller output is lost, then the previous plant input is held:

$$
\begin{aligned}
x_{k+1} &= Ax_k + \Gamma_k^{(10)}BL\hat{x}_k^s + (1 - \Gamma_k^{(10)})Bu_{k-1} + w_k, \\
\hat{x}_k^s &= A\hat{x}_{k-1}^s + B\hat{u}_{k-1}^s \\
&\quad + K\big(y_k - C(A\hat{x}_{k-1}^s + B\hat{u}_{k-1}^s)\big),
\end{aligned}
\tag{32}
$$

where $\Gamma_k^{(10)}$ is as in (7) and

$$
\hat{u}_{k-1}^s = \begin{cases} u_{k-1} & \text{if } \delta_{k-1}^{(1)} = 1, \\ L\hat{x}_{k-1}^s & \text{if } \delta_{k-1}^{(1)} = 0. \end{cases}
$$

Independent and identically distributed dropouts: We first consider i.i.d. transmission processes as per Assumption 1. Fig. 3 illustrates a histogram of c_k, obtained by running the algorithm for 1000 steps with dropout probabilities as indicated. Whilst (18) shows that for small p, control calculations are at most times, carried out at the actuator node, Fig. 3 illustrates that if links are more reliable, then the controller will be placed at the sensor node at most time steps.

We first consider a noiseless unstable plant model (1), where

$$
A = \begin{bmatrix} 1.87 & -0.86 \\ 1 & 0 \end{bmatrix}, \; B = \begin{bmatrix} 1 \\ 0 \end{bmatrix}, \; C = \begin{bmatrix} 0.048 & 0.045 \end{bmatrix}
\tag{33}
$$

with Gaussian initial state having mean $\bar{x}_0 = [5 \quad 5]^T$ and covariance $P_0 = 0.1 \times I_2$. Controller and estimator gains L and K correspond to the steady state LQG/LQR controller with stage cost $\|x_k\|^2 + \|u_k\|^2/10$. All nodes use as initial

state estimates, $\hat{x}_0^{(i)} = [0 \quad 0]^T$. The network has i.i.d. dropouts with success probabilities $p = 0.9$ and $q_1 = \cdots = q_9 = 1$.

The baseline NCS (32) failed to stabilize the present system. Fig. 4 compares a typical plant output trajectory obtained by using the proposed algorithm (solid line) with that provided by the baseline NCS (31) (dashed line). As can be appreciated, the adaptive controller allocation algorithm presented reacts more quickly to plant outputs. It thereby recovers more quickly from the very bad local initial state estimates and provides control actions leading to faster convergence to the origin. If we adopt the empirical performance measure

$$
J \triangleq \sum_{k=1}^{1000} y_k^2,
\tag{34}
$$

then, with the dynamic architecture, we obtain $J \approx 3$, whereas for the baseline NCS described by (31), $J \approx 11$.

We next consider a plant model with an integrator, where

$$
A = \begin{bmatrix} 1.8 & -0.8 \\ 1 & 0 \end{bmatrix}, \; Q = 0.01 \times I_2, \; R = 0.01
\tag{35}
$$

and B and C as in (33). The initial state has mean $\bar{x}_0 = [10 \quad 10]^T$. Table II illustrates how the performance gained by using the proposed method depends upon the network reliability. For the situation examined, larger performance gains are obtained with smaller p. For larger p, the performance gains become less relevant. This finding is intuitive, since for $p \approx 1$ the network becomes transparent and overall performance is dominated by the nominal design (1)–(3).

Network with moving obstacle: We now focus on a network with an obstacle (e.g., a robot or crane) moving between four different positions, see Fig. 5. We model this as in Section VI, using the network state process $\Xi_k \in \mathbb{B} = \{1, 2, 3, 4\}$. The transition probabilities for Ξ_k are given by:

$$
[p_{ij}] = \begin{bmatrix} 0.99 & 0.01 & 0 & 0 \\ 0.003 & 0.99 & 0.007 & 0 \\ 0 & 0.003 & 0.99 & 0.007 \\ 0.007 & 0 & 0.003 & 0.99 \end{bmatrix}.
$$

The individual link reliabilities depend on the position of the obstacle. Nodes which are not blocked benefit from high success probabilities $r \in [0.88, 1]$. Due to the obstacle, some of the success probabilities will, at times, be lowered to 60%:
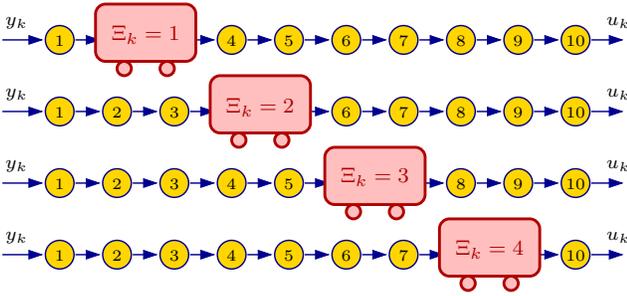
Fig. 5. Sensor-actuator network with moving obstacle.
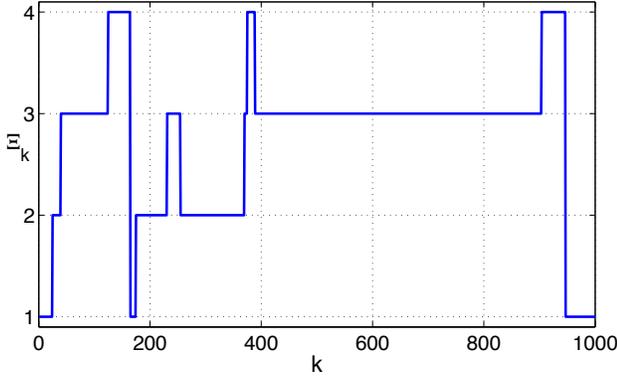
Fig. 6. Network state trajectory, Ξ_k.
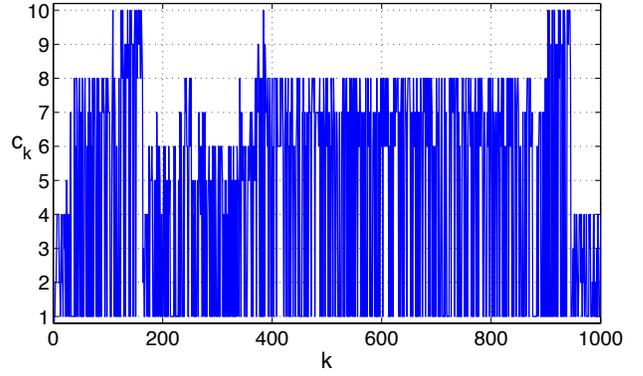
Fig. 7. Controller location c_k for the network in Fig. 5.
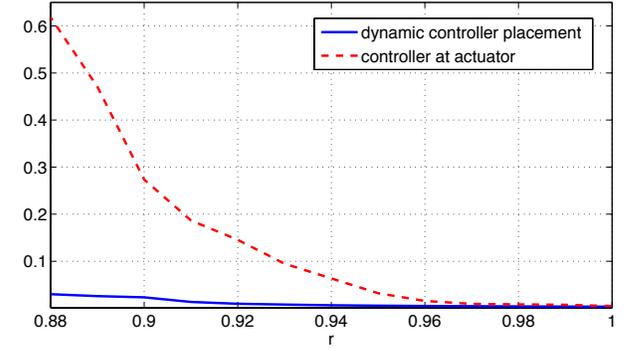
Fig. 8. Trace of the stationary covariance of the plant state x_k in (35) as a function of the success probability r, see (36).

$$\mathbf{Pr}\{\gamma_k^{(i)} = 1 \,|\, \Xi_k = j\} = \begin{cases} 0.6 & \text{if } i \in \{2j-1, 2j, 2j+1\} \\ r & \text{in all other cases} \end{cases}$$

$$\mathbf{Pr}\{\delta_{k-1}^{(i)} = 1 \,|\, \Xi_k = j\} = \begin{cases} 0.6 & \text{if } i \in \{2j, 2j+1\} \\ r & \text{in all other cases.} \end{cases}$$
(36)

For $r = 0.99$, Figs. 6 and 7 illustrate how using Algorithm 1 the controller location depends upon the network state Ξ_k. It turns out that, in the present case, the plant input is always provided by one of the nodes located between the sensor node and the node immediately following the blocked ones. This behaviour can be explained by noting that, in absence of the obstacle, the network is very reliable. In fact, if none of the nodes were blocked, then the algorithm would (almost) always locate the controller at the sensor node.

For (35) and with $r = 0.99$, use of the dynamic architecture proposed, gave $J = 51.6$. In contrast, if the controller is fixed at the actuator node, see (31), then $J = 68.5$ was obtained. This amounts to a performance loss of 33%. In the situations examined, positioning the baseline NCS (32) failed to stabilize the plant model. Fig. 8, obtained using Theorem 1, illustrates how the trace of the covariance of the plant state (35) depends on the network parameter r in (36). In this figure, the solid line corresponds to the dynamic controller placement method, whereas the dashed line refers to the baseline controller (31). Our results clearly indicate that, without the need for controller re-design, the algorithm proposed in the present work has the potential to give significant performance gains when compared to earlier NCS configurations where node functionalities are fixed.

VIII. CONCLUSIONS

We have presented a flexible architecture for the implementation of a linear control law over a wireless sensor-actuator network using analog erasure channels without acknowledgments. With the algorithm provided, the role played by individual nodes depends on transmission outcomes. In particular, the controller location is adapted to the availability of past plant input values and transmission outcomes. By deriving a Markovian jump-linear system model, we established a closed form expression for the stationary covariance of the system state in the presence of correlated dropout processes. Future work may include extending the ideas to multiple-loops, to general network topologies, and to controller design.

REFERENCES

[1] D. E. Quevedo, A. Ahlén, and K. H. Johansson, "Stability of state estimation over sensor networks with Markovian fading channels," in *Proc. IFAC World Congr.*, 2011.

[2] P. Antsaklis and J. Baillieul, "Special issue on technology of networked control systems," *Proc. IEEE*, vol. 95, no. 1, pp. 5–8, Jan. 2007.

[3] J. Chen, K. H. Johansson, S. Olariu, I. C. Paschalidis, and Stokmenovic, "Guest editorial special issue on wireless sensor and actuator networks," *IEEE Trans. Automat. Contr.*, vol. 56, no. 11, pp. 2244–2246, Oct. 2011.

[4] G. C. Goodwin, D. E. Quevedo, and E. I. Silva, "Architectures and coder design for networked control systems," *Automatica*, vol. 44, no. 1, pp. 248–257, Jan. 2008.

[5] C. L. Robinson and P. R. Kumar, "Optimizing controller location in networked control systems with packet drops," *IEEE J. Select. Areas Commun.*, vol. 26, no. 4, pp. 661–671, May 2008.

[6] M. Pajic, S. Sundaram, G. J. Pappas, and R. Mangharam, "The wireless control network: A new approach for control over networks," *IEEE Trans. Automat. Contr.*, vol. 56, no. 10, pp. 2305–2318, Oct. 2011.

[7] D. Nešić and A. R. Teel, "Input-to-state stability of networked control systems," *Automatica*, vol. 40, pp. 2121–2128, 2004.

[8] M. C. F. Donkers, W. P. M. H. Heemels, N. van de Wouw, and L. Hetel, "Stability analysis of networked control systems using a switched linear systems approach," *IEEE Trans. Automat. Contr.*, vol. 56, no. 9, pp. 2101–2115, Sept. 2011.

[9] D. Antunes, J. Hespanha, and C. Silvestre, "Stability of networked control systems with asynchronous renewal links: An impulsive systems approach," *Automatica*, vol. 49, no. 2, pp. 402–413, Feb. 2013.

[10] D. E. Quevedo, A. Ahlén, and K. H. Johansson, "State estimation over sensor networks with correlated wireless fading channels," *IEEE Trans. Automat. Contr.*, vol. 58, no. 3, pp. 581–593, Mar. 2013.

[11] D. E. Quevedo, K. H. Johansson, A. Ahlén, and I. Jurado, "Dynamic controller allocation for control over erasure channels," in *Proc. 3rd IFAC Workshop on Distributed Estimation and Control in Networked Systems*, Santa Barbara, CA, 2012.

[12] O. C. Imer, S. Yüksel, and T. Başar, "Optimal control of LTI systems over unreliable communication links," *Automatica*, vol. 42, no. 9, pp. 1429–1439, Sept. 2006.

[13] A. Chiuso and L. Schenato, "Information fusion strategies and performance bounds in packet-drop networks," *Automatica*, vol. 47, pp. 1304–1316, July 2011.

[14] M. Huang and S. Dey, "Stability of Kalman filtering with Markovian packet losses," *Automatica*, vol. 43, no. 4, pp. 598–607, Apr. 2007.

[15] D. E. Quevedo, A. Ahlén, and J. Østergaard, "Energy efficient state estimation with wireless sensors through the use of predictive power control and coding," *IEEE Trans. Signal Processing*, vol. 58, no. 9, pp. 4811–4823, Sept. 2010.

[16] D. E. Quevedo, A. Ahlén, A. S. Leong, and S. Dey, "On Kalman filtering over fading wireless channels with controlled transmission powers," *Automatica*, vol. 48, no. 7, pp. 1306–1316, July 2012.

[17] O. L. V. Costa, M. D. Fragoso, and R. P. Marques, *Discrete-Time Markov Jump Linear Systems*. London, U.K.: Springer-Verlag, 2005.

[18] J.-W. Lee and G. E. Dullerud, "A stability and contractiveness analysis of discrete-time Markovian jump linear systems," *Automatica*, vol. 43, no. 1, pp. 168–173, Jan. 2007.

[19] P. Lancaster, "Explicit solutions of linear matrix equations," *SIAM Review*, vol. 12, no. 4, pp. 544–566, Oct. 1970.

APPENDIX

With Assumption 1, $\mathbf{Pr}\{\mu_k^{(1)} = 1\} = \mathbf{Pr}\{\delta_{k-1}^{(1)} = 1\} = q_1$. It is easy to see from lines 11 and 27 of Algorithm 1 that

$$
\begin{aligned}
i \in \mathcal{C}_k &\Longleftrightarrow \delta_{k-1}^{(i)} = 1 \\
&\wedge \left(\gamma_k^{(i-1)} = 0 \vee \left(\gamma_k^{(i-1)} = 1 \wedge \mu_k^{(i-1)} = 0\right)\right) \quad (37) \\
&\Longleftrightarrow \delta_{k-1}^{(i)} = 1 \wedge \left(\gamma_k^{(i-1)} = 0 \vee \mu_k^{(i-1)} = 0\right)
\end{aligned}
$$

and that, similarly

$$
\begin{aligned}
\mu_k^{(i)} = 0 &\Longleftrightarrow \left(\gamma_k^{(i-1)} = 0 \wedge \delta_{k-1}^{(i)} = 0\right) \\
&\vee \left(\gamma_k^{(i-1)} = 1 \wedge \mu_k^{(i-1)} = 0 \wedge \delta_{k-1}^{(i)} = 0\right) \\
&\Longleftrightarrow \delta_{k-1}^{(i)} = 0 \quad (38) \\
&\wedge \left(\gamma_k^{(i-1)} = 0 \vee \left(\gamma_k^{(i-1)} = 1 \wedge \mu_k^{(i-1)} = 0\right)\right) \\
&\Longleftrightarrow \delta_{k-1}^{(i)} = 0 \wedge \left(\gamma_k^{(i-1)} = 0 \vee \mu_k^{(i-1)} = 0\right)
\end{aligned}
$$

for all $i \in \{1, 2, \ldots, M\}$. (38) provides the recursion

$$
\begin{aligned}
\mathbf{Pr}\{\mu_k^{(i)} = 1\} &= 1 - \mathbf{Pr}\{\delta_{k-1}^{(i)} = 0\} \\
&\quad \times \mathbf{Pr}\{\mu_k^{(i-1)} = 0 \vee \gamma_k^{(i-1)} = 0\} \\
&= 1 - (1 - q_i)\left(1 - \mathbf{Pr}\{\mu_k^{(i-1)} = 1 \wedge \gamma_k^{(i-1)} = 1\}\right) \\
&= 1 - (1 - q_i)\left(1 - p\mathbf{Pr}\{\mu_k^{(i-1)} = 1\}\right) \\
&= q_i + p(1 - q_i)\mathbf{Pr}\{\mu_k^{(i-1)} = 1\},
\end{aligned}
$$

having explicit solution (15). On the other hand, (37) gives

$$
\begin{aligned}
&\mathbf{Pr}\{i \in \mathcal{C}_k\} \\
&= \mathbf{Pr}\{\delta_{k-1}^{(i)} = 1\}\left(1 - \mathbf{Pr}\{\gamma_k^{(i-1)} = 1\}\mathbf{Pr}\{\mu_k^{(i-1)} = 1\}\right),
\end{aligned}
$$

thus establishing (16). By (11) we obtain

$$
\begin{aligned}
\mathbf{Pr}\{c_k = i\} &= \mathbf{Pr}\{\max(\mathcal{C}_k) = i\} \\
&= \mathbf{Pr}\{i \in \mathcal{C}_k \wedge \gamma_k^i = \gamma_k^{i+1} = \cdots = \gamma^{M-1} = 1\}
\end{aligned}
$$

for $i \in \{1, \ldots, M - 1\}$, whereas for the actuator node, we have $\mathbf{Pr}\{c_k = M\} = \mathbf{Pr}\{M \in \mathcal{C}_k\}$. This proves (17). $\square$

By the law of total expectation, we have

$$
\mathbf{E}\{\Theta_{k+1}\Theta_{k+1}^T\} = \sum_{i \in \mathbb{B}} H_{k+1,i}, \quad (39)
$$

where

$$
H_{k+1,i} \triangleq \mathbf{E}\{\Theta_{k+1}\Theta_{k+1}^T \,|\, \Xi_k = i\}\mathbf{Pr}\{\Xi_k = i\}. \quad (40)
$$

Now, the system equation (27) together with the network fading model in Assumption 2 allow one to write

$$
\begin{aligned}
\mathbf{E}\{\Theta_{k+1}\Theta_{k+1}^T \,|\, \Xi_k = i\} &= \mathbf{E}\{(\mathcal{A}(\beta_k)\Theta_k + \mathcal{B}(\beta_k)n_k) \\
&\quad \times (\mathcal{A}(\beta_k)\Theta_k + \mathcal{B}(\beta_k)n_k)^T \,|\, \Xi_k = i\} \\
&= \mathbf{E}\{\mathcal{A}(\beta_k)\Theta_k\Theta_k^T\mathcal{A}(\beta_k)^T \,|\, \Xi_k = i\} \quad (41) \\
&\quad + \mathbf{E}\{\mathcal{B}(\beta_k)n_k n_k^T\mathcal{B}(\beta_k)^T \,|\, \Xi_k = i\} \\
&= \mathbf{E}\{\mathcal{A}(\beta_k)\Theta_k\Theta_k^T\mathcal{A}(\beta_k)^T \,|\, \Xi_k = i\} + \overline{\mathcal{B}}_i W (\overline{\mathcal{B}}_i)^T
\end{aligned}
$$

since $\{n_k\}$ is zero-mean i.i.d. The rule of total expectation, Bayes' rule and the Markovian property of (27) give that

$$
\begin{aligned}
&\mathbf{E}\{\mathcal{A}(\beta_k)\Theta_k\Theta_k^T\mathcal{A}(\beta_k)^T \,|\, \Xi_k = i\} \\
&= \sum_{j \in \mathbb{B}} \mathbf{E}\{\mathcal{A}(\beta_k)\Theta_k\Theta_k^T\mathcal{A}(\beta_k)^T \,|\, \Xi_k = i, \Xi_{k-1} = j\} \\
&\quad \times \mathbf{Pr}\{\Xi_{k-1} = j \,|\, \Xi_k = i\} \quad (42) \\
&= \sum_{j \in \mathbb{B}} \mathbf{E}\{\mathcal{A}(\beta_k)\Theta_k\Theta_k^T\mathcal{A}(\beta_k)^T \,|\, \Xi_k = i, \Xi_{k-1} = j\} \\
&\quad \times \mathbf{Pr}\{\Xi_k = i \,|\, \Xi_{k-1} = j\}\mathbf{Pr}\{\Xi_{k-1} = j\}/\mathbf{Pr}\{\Xi_k = i\} \\
&= \sum_{j \in \mathbb{B}} p_{ji}\overline{\mathcal{A}}_i\mathbf{E}\{\Theta_k\Theta_k^T \,|\, \Xi_{k-1} = j\}(\overline{\mathcal{A}}_i)^T \frac{\mathbf{Pr}\{\Xi_{k-1} = j\}}{\mathbf{Pr}\{\Xi_k = i\}}.
\end{aligned}
$$

Substitution of (42) into (41) and then into (40) provides

$$
\begin{aligned}
H_{k+1,i} &= \sum_{j \in \mathbb{B}} p_{ji}\overline{\mathcal{A}}_i\mathbf{E}\{\Theta_k\Theta_k^T \,|\, \Xi_{k-1} = j\}(\overline{\mathcal{A}}_i)^T \quad (43) \\
&\quad \times \mathbf{Pr}\{\Xi_{k-1} = j\} + \overline{\mathcal{B}}_i W (\overline{\mathcal{B}}_i)^T\mathbf{Pr}\{\Xi_k = i\} \\
&= \sum_{j \in \mathbb{B}} p_{ji}\overline{\mathcal{A}}_i H_{k,j}(\overline{\mathcal{A}}_i)^T + \overline{\mathcal{B}}_i W (\overline{\mathcal{B}}_i)^T\mathbf{Pr}\{\Xi_k = i\}
\end{aligned}
$$

Since the NCS is assumed MSS, it is asymptotically wide-sense stationary [17, Thm. 3.33]. If we define $H_i \triangleq \lim_{k \to \infty} H_{k,i}$, $i \in \mathbb{B}$, and recall that $\{\Xi_k\}$ is aperiodic, then (43) becomes (30), and (39) establishes (29). $\qquad \square$